LEGIBILITY NOTICE

A major purpose of the Technical Information Center is to provide the broadest dissemination possible of information contained in DOE's Research and Development Reports to business, industry, the academic community, and federal, state and local governments.

Although a small portion of this report is not reproducible, it is being made available to expedite the availability of information on the research discussed herein.

Los Alamos National Laboratory is operated by the University of California for the United States Department of Energy under contract W-7405-ENG-36

TITLE *THE ALEXIS PROJECT AND THE LOCAL INTERSTELLAR MEDIUM*

LA-UR--89-1077

DE89 009246

AUTHOR(S) *J. J. Bloch and B. W. Smith, ESS-9*

SUBMITTED TO *Proceedings of the Berkeley Colloquium on Extreme Ultraviolet Astronomy, University of California, Berkeley, January 18-21, 1989*

DISCLAIMER

3/89

Los Alamos National Laboratory
Los Alamos, New Mexico 87545

The ALEXIS Project and the Local Interstellar Medium

J. J. Bloch and Barham W. Smith
Space Astronomy and Astrophysics Group
Los Alamos National Laboratory, Los Alamos, NM, USA

ABSTRACT

The ALEXIS satellite (Priedhorsky *et al.*, this volume) will be a valuable tool for studying the diffuse soft X-ray background (SXRB). The SXRB emission (0.07-0.25 keV) is thought to originate in a plasma at about 10^6K that exists in the local interstellar medium. Emission models of such a plasma (Raymond and Smith 1977,1987) with normal cosmic elemental abundances predict that about 34% of the atomic cooling power comes from a set of closely-spaced lines around 70 eV from Fe VII through XII. Two passbands of the ALEXIS telescopes will be centered at 66 and 72 eV to include the Fe line emission. The flux from these lines in the SXRB could produce a signal of as much as 150 counts per second for ALEXIS telescopes with these passbands. With the narrow spectral response of the ALEXIS telescopes, an unambiguous measurement of the flux from the lines will be possible. When combined with other data sets, the intensities of the SXRB in the 66 and 72 eV bands allow distinction between models of emission from hot gas having normal and depleted abundances. ALEXIS' spatial resolution and estimated year-long operating lifetime will allow the generation of all-sky maps of the SXRB in these Fe lines with about one degree resolution and considerable sensitivity. These maps will be more sensitive to absorption features due to nearby low-column-density clouds than maps done in higher energy bands.

I. Introduction

In this paper we explore the scientific harvest of the ALEXIS satellite (Priedhorsky et al., 1988, 1989) relating to the local interstellar medium (LISM). After its discovery (Bowyer, Field, and Mack 1968), the origin of the soft X-ray background (SXRB) remained a mystery, until it was recognized as the signature of a component of the ISM at about 10^6K. The LISM is thought to be largely comprised of a thin plasma with a temperature between 8×10^5K and 1.5×10^6K. The ultrasoft X-ray background has never been mapped with the angular resolution expected from ALEXIS, nor with the narrow band selectivity of metal multilayer mirrors. The key to understanding the origin and nature of this phase of the ISM lies in both spatial and spectral studies of its soft X-ray and EUV emission.

ALEXIS will be able to perform such studies of the SXRB. It consists of 6 ultrasoft X-ray telescopes working at near normal incidence with microchannel plate detectors. Each telescope will have a 33 degree field of view and an effective collecting area of approximately 0.5 cm^2, including all efficiency factors. FWHM spectral resolution of the mirrors will be ~5%. The telescopes will utilize spherical mirrors coated with layered synthetic microstructures (LSMs) tuned to three narrow passbands distributed among six telescopes. By carefully selecting two of the telescope passbands to lie on top of relatively intense EUV emission lines, the ratios of the fluxes detected in the different bands will be an important tool for temperature and elemental abundance determinations. This is described in the first section below. The second section below describes how the angular resolution of the ALEXIS telescopes will provide improved constraints on spatial models of the distribution of the X-ray emitting gas within the local interstellar medium.

II. ALEXIS as a Tool for Abundance and Temperature Diagnostics

Ability to distinguish between alternative models of the LISM drives the choice of energy bands for the ALEXIS telescopes. Each mirror will have a bandwidth of acceptance of only about 8 angstroms, determined by the characteristics of its LSM and by the restricted range of reflection angles allowed by

the geometry of the optical system. Within each 8 angstrom band, reflectivities for individual spectral lines vary according to their differing wavelengths. Reflectivity at wavelengths outside the bandwidth of a mirror is low enough that it can be neglected, since the mirrors are tuned to spectral regions containing the strongest lines, and there are no stronger lines just outside. However, there is some overlap between the 66 eV and 72 eV responses that must be considered. The net response of one mirror to the line-rich spectrum expected from the LISM is the sum of the responses to individual spectral lines within its bandwidth. Thus the scientific products of the ALEXIS all-sky survey of the LISM will be band intensities and band ratios. Can we distinguish between models of the LISM using this information?

We have computed the expected flux in all the spectral lines arising in a hot plasma that fall within each bandwidth, using the Raymond and Smith (1987) plasma spectrum code (see Fig. 9 of Priedhorsky *et al.* 1989). The expected flux is normalized to the Be (beryllium) band (70 to 111 eV) measurements of the Wisconsin soft X-ray survey (Bloch *et al.* 1986, Bloch 1988). We tabulate the expected band intensities for a range of temperatures and for both normal and depleted (Spitzer and Jenkins 1975) abundance sets. Depleted plasmas whose normalized emission provides enough Be band counts require more emission measure than plasmas with normal abundances. Thus the observed spectrum of depleted plasmas contains stronger oxygen and neon lines than that of normal abundance plasmas, whose emission in the ALEXIS bands is largely due to iron.

The reflectivity of a LSM is such a strong function of incidence angle on the mirror that adjacent lines in the spectrum of a hot plasma have different integrated reflectivities. For the current ALEXIS optical design, incoming rays sample a range of normal incidence angles from 12.3 to 17.7 degrees. The area-solid-angle product of this optical system for each spectral line is found from the convolution of the differential area-solid-angle product (as a function of incidence angle) with the reflectivity as a function of incidence angle. In the tables that follow, we give this number in cm^2 sr for each line.

The emissivity of a hot plasma can be given in erg cm^3/sec (e.g. Raymond and Smith 1987), but to ease normalization to the Wisconsin Be band flux it can instead be given as photons cm^2 sr EM, where EM is the emission measure along a typical line of sight in cm^{-6} pc. When the emissivity from a spectral line is multiplied by the area-solid-angle product for that line and by the EM required to produce the Wisconsin Be band count rate, an estimated number of photons per second results. This photon rate is the rate reflected off the mirror and toward the ALEXIS filter/detector system, which will have a net efficiency of about 0.25, so the actual count rates will be about 1/4 the photon rates tabulated here. In Tables 1 through 4 we give these photon rates for the three ALEXIS bands and for the two cases of normal and depleted abundances in the LISM. The range of log(T) shown, from 5.8 to 6.2, includes all temperatures for the LISM that are consistent with intensity ratios of the B (boron, 130 to 188 eV) and C (carbon, 160 to 284 eV) bands from the Wisconsin survey. Most of the emitting gas must be within this temperature range, although small volumes may depart from it.

Table 1: Lines Contributing to 66 eV Band, Normal Abundances

	Line		A Ω	log(T)				
Ion	E(eV)	λ(A)	cm^2 sr	5.8	5.9	6.0	6.1	6.2
Fe VII	66.95	185.2	1.71	16800	10400	1900	200	0
O VI	67.35	184.1	1.67	1500	800	700	0	0
Fe XI	68.73	180.4	1.19	500	5000	24000	37800	15500
Fe XII	66.34	186.9	1.60	0	800	11700	43700	44600
Ar XI	65.67	188.8	1.14	0	0	0	700	1400
S XI	64.85	191.2	0.51	0	0	0	0	500
Totals				18800	17000	40300	86700	62000
EM required (cm^{-6} pc)				004	005	008	002	01
Photons per sec (from mirror)				75	85	202	607	620

Table 2: Lines Contributing to 66 eV Band, Depleted Abundances

Line			$A\,\Omega$	log(T)				
Ion	E(eV)	λ(A)	cm^2-sr	5.8	5.9	6.0	6.1	6.2
O VI	67.35	184.1	1.67	1120	650	450	380	330
Fe VIII	66.95	185.2	1.71	210	130	50	0	0
Fe XI	68.73	180.4	1.19	0	60	300	480	190
Fe XII	66.34	186.9	1.60	0	0	150	300	560
S XI	64.85	191.2	0.51	0	0	0	70	240
Ar XI	65.67	188.8	1.14	0	0	0	100	280
Totals				1330	840	950	1630	1600
EM required (cm^{-6}-pc)				.008	.02	.04	.05	.05
Photons per sec(from mirror)				11	17	38	82	80

Table 3: Lines Contributing to 72 eV Band, Normal Abundances

Line			$A\,\Omega$	log(T)				
Ion	E(eV)	λ(A)	cm^2-sr	5.8	5.9	6.0	6.1	6.2
Fe IX	72.47	171.1	1.99	59900	75400	53400	15600	1400
Fe X	71.01	174.6	1.96	12100	44000	78000	51000	9600
O VI	71.67	173.0	2.08	3300	2000	1400	1200	1100
Fe VII	70.17	176.7	1.34	800	0	0	0	0
Totals				76100	121400	132800	67800	12100
EM required (cm^{-6} pc)				.004	.005	.005	.007	.01
Photons per s(from mirror)				300	610	660	470	120

Table 4: Lines Contributing to 72 eV Band, Depleted Abundances

Line			$A\,\Omega$	log(T)				
Ion	E(eV)	λ(A)	cm^2 sr	5.8	5.9	6.0	6.1	6.2
O VI	71.67	173.0	2.08	2540	1490	1080	920	810
Fe IX	72.47	171.1	1.99	760	950	670	200	20
Ne V	71.30	173.9	2.02	230	0	0	0	0
Fe X	71.01	174.6	1.96	150	550	980	640	120
Totals				3680	2990	2710	1760	950
EM required (cm^{-6} pc)				.008	.02	.04	.05	.05
Photons per sec(from mirror)				29	60	108	88	48

In Figure 1 we display the two band photon rates (not including the efficiency of the filter and detector system) as a function of temperature and depletion. For gas temperatures greater than about 10^6K there is clear separation between variations in temperature and in depletion. However for the lower temperatures there will be a residual ambiguity which may be resolved by the Be/B and B/C ratios (see Bloch 1988). Note that the (72 eV)/(66 eV) band ratio is insensitive to absorption by cold gas, because the band energies are so close. A bandpass centered at 83 eV has also been considered, since it encompasses several moderately strong neon and oxygen lines, as well as some nickel lines analogous to the iron lines in the lower bandpasses. However, this band does little to resolve the ambiguity at lower temperature. The third ALEXIS bandpass will be centered at about 95 eV and does not encompass any significant emission lines expected from the LISM. It will serve, nevertheless, as a check on the other bands.

III. Spatial Studies of the SXRB with ALEXIS

The SXRB has been mapped in the C, B, and Be bands with spatial resolution ranging from 3 degrees

to 15 degrees (Bloch *et al* 1986, Bloch 1988, Marshall and Clark 1984, McCammon *et al* 1983). These maps have been used as the basis for models of the distribution of hot X-ray emitting material and absorbing neutral clouds in the interstellar medium. Figure 2 shows the column density as a function of photon energy for one optical depth through the neutral phase of the interstellar medium. The centers of the ALEXIS telescope bandpasses are indicated with vertical dotted lines. The top horizontal dashed line shows the minimum HI column density out of the Galaxy towards the north galactic pole. The second dashed line indicates the approximate column density of neutral interstellar material estimated to be between the Sun and the wall of the local cavity. As can be seen from this plot, the ALEXIS bandpasses will be sensitive to fluctuations in the SXRB flux caused by nearby clouds of relatively low column density. The Sun appears to be inside such a cloudlet. How many similar cloudlets are inside of the local cavity? Comparing maps of the SXRB in the ALEXIS bandpasses with higher energy maps could help to describe the local distribution of these low column density clouds.

To demonstrate this, we have simulated observations of the SXRB flux from a model cavity. We have filled a sphere with a radius of 100 pc with hot X-ray emitting gas of uniform emissivity and placed spherical clouds randomly within it. For the model shown, the radius of the clouds was 3 pc and their column density through the center was $N_{HI}=2\times10^{18}cm^{-2}$. The cloud density is approximately $0.01pc^{-3}$. This model is not put forth as a candidate description of the local ISM, but rather as a demonstration of the information content in the SXRB spatial maps that will be generated by ALEXIS. Figure 3 contains four simulated map sections of the SXRB at different energies arranged as quadrants of a Hammer-Aitoff map projection. The resolution of the maps is 2.0 degrees. However, the ultimate resolution possible with ALEXIS should be in the range of 1.0 to 0.5 degrees. The upper right quadrant of the map shows the model sky as it would be seen by the 72 eV ALEXIS telescopes. The upper left quadrant shows the sky as it would appear to the 95 eV ALEXIS telescopes (95 eV is also the average energy of the Be band). The bottom right quadrant shows the model sky as it would appear in the B band (130 - 188 eV), and the bottom left quadrant as it would appear in the C band (160 - 284 eV). C band maps which surpass this spatial quality will be produced by ROSAT.

As can be seen in the figure, the fluctuations due to absorption increase as the photon energy of the observation drops. Modeling of such spatial fluctuations in the actual SXRB spatial data from ALEXIS, ROSAT and other existing data sets will put constraints on local cloud distribution models. Intensity minima seen in maps like these can be due either to absorption of distant flux by nearer cold gas (see e.g. Jakobsen and Kahn 1986) or to absence of flux due to shorter lines of sight through the hot gas (e.g. Cox and Snowden 1986, Bloch 1988). Intensity maxima can arise through variations in temperature or through longer lines of sight through hot gas. Important constraints on models have been developed by comparing Be, B, and C band maps of the sky. For example, while the data used to generate these ratios was obtained mostly from maps with >6 degree fields of view, ALEXIS and ROSAT will usher in a new era when such maps can be generated on scales better than one degree. As more mapping of clouds in the LISM occurs (York and Frisch 1989), there is hope that specific neutral structures can be associated with features in ALEXIS maps to better describe our local interstellar environment.

IV. Conclusions

ALEXIS will provide a wealth of data on the SXRB. The spatial maps produced by ALEXIS when combined with other data sets will give us valuable information on the distribution of hot X-ray emitting plasma and cold absorbing diffuse clouds in the local vicinity of the Sun. The flux measured in ALEXIS' narrow energy bandpasses will help constrain models of the x-ray emission from the plasma. The conclusions drawn from these two types of studies will help us discover the nature and origin of the hot phase of the interstellar medium.

This work is supported by the Department of Energy.

References

Bowyer, C. S., Field, G. B., and Mack, J. E. 1968, *Nature*, 217, 32.

Bloch, J. J., Jahoda, K., Juda, M., McCammon, D., Sanders, W. T., and Snowden, S. L. 1986, *Ap. J. (Letters)*, 308, L59.

Bloch, J. J. 1988, Ph.D. thesis, University of Wisconsin-Madison

Cox, D. P., and Snowden, S. L. 1986, *Adv. Space Res.*, 6, 97.

Jakobsen, P., and Kahn, S. M. 1986, *Ap. J.*, 309, 682

Marshall, F. J., and Clark, G. W. 1984, *Ap. J.*, 287, 633

McCammon, D., Burrows, D. N., Sanders, W. T., and Kraushaar, W. L. 1983, *Ap. J.*, 269, 107

Priedhorsky, W. C., Bloch, J. J., Smith, B. W., Strobel, K., Ulibarri, M., Chavez, J., Evans, E., Siegmund, O. H. W., Marshall, H., Vallerga, J., and Vedder, P., *X-ray Instrumentation in Astronomy*, SPIE Proceedings, 982, 1988.

Priedhorsky, W. C., Bloch, J. J., Cordova, F., Smith, B. W., Strobel, K., Ulibarri, M., Chavez, J., Evans, E., Siegmund, O. H. W., Marshall, H., Vallerga, J., and Vedder, P., 1989, this volume

Raymond, J. C., and Smith, B. W. 1977, *Ap. J. Suppl.*, 35, 419.

—. 1987, *private communication* (update to Raymond and Smith 1977)

Spitzer, L., and Jenkins, E. B. 1975, *Ann. Rev. Astr. Ap.*, 13, 133

York, D. G., and Frisch, P. C. 1989, this volume

Figure Captions

Figure 1 — Rates of photons reflected off the mirrors toward the filters, for the 66 eV and 72 eV ALEXIS bandpasses. The data plotted is taken from the accompanying tables. The solid line connects points for normal abundances, and the dotted line connects those for depleted abundances. Each point is labeled by the log of the gas temperature.

Figure 2 – Plot of column density through the neutral interstellar medium required to achieve an optical depth of one as a function of photon energy. The minimum column density out of the galaxy is indicated, as well as the estimated typical column density along a line of sight to the wall of the local cavity. The four vertical dotted lines indicate the centers of the proposed ALEXIS telescope bandpasses.

Figure 3 — Simulated maps of the soft X-ray background from the center of a mythical cavity in the ISM filled with x-ray emitting plasma. Spherical clouds of absorbing neutral material have been placed randomly within the cavity with an average cloud density of $0.01 pc^{-3}$. The clouds are all of the same size with radii of 3 pc, and column densities through their centers of N_{HI} $2\times10^{18} cm^{-2}$. Each quadrant of the mapoff map is a section of the simulated soft X-ray background emission at different energies. The upper right corner of the map is a simulated map made at 72 eV, one of the ALEXIS bandbasses. The upper left quadrant is a map made at 95 eV, which

is one of the ALEXIS bandpasses and also the average photon energy within the Be Band. The bottom right map shows how the cavity would appear in the B band, and the bottom left in the C band. The maps have all been displayed with the same contour and greyscale levels, and the plasma emissivity for all wavelengths are assumed to be the same for this comparison. The magnitude of the fluctuations varies from 50% at 72 eV to about 5% at C band energies.

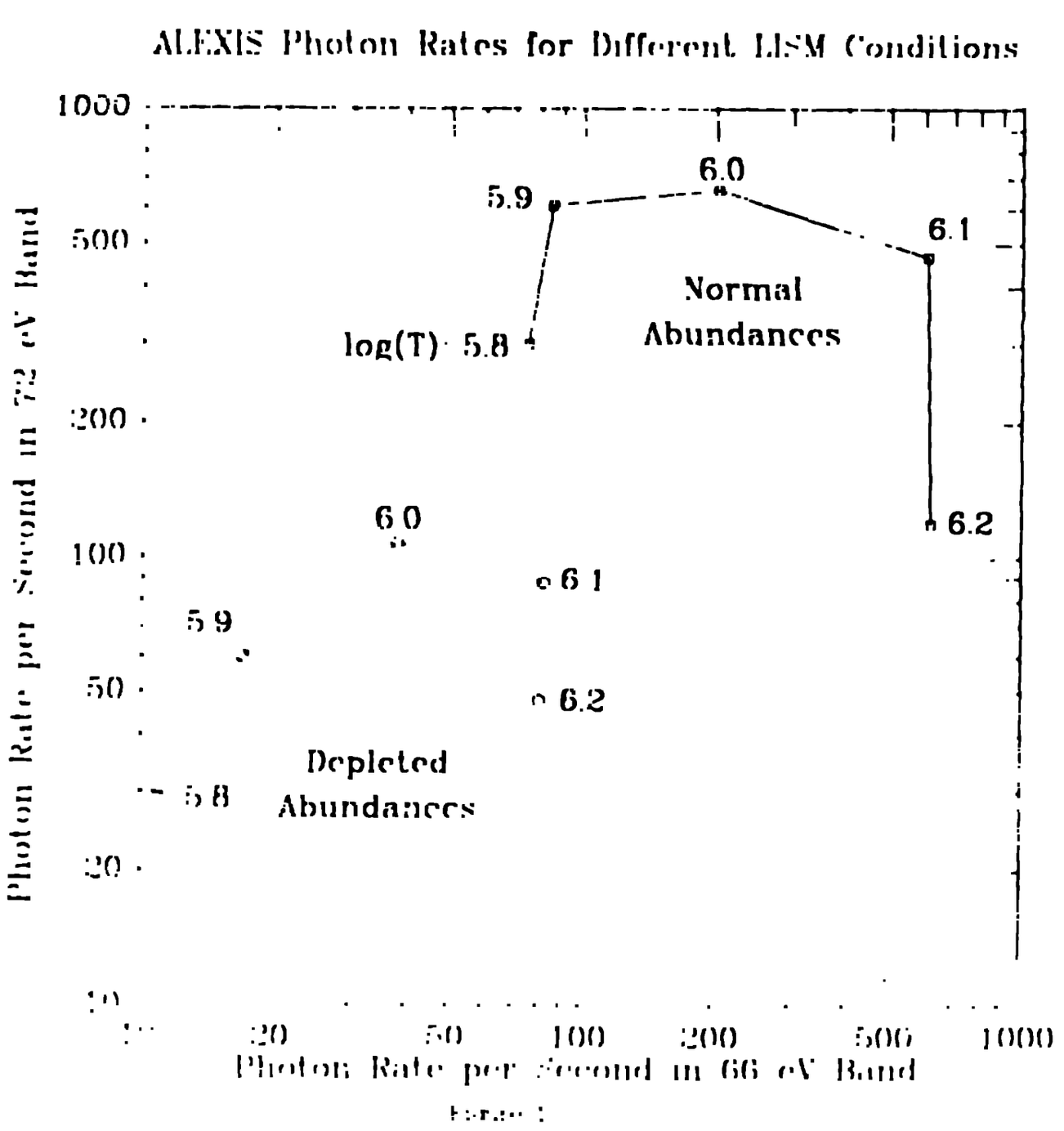
ALEXIS Photon Rates for Different LISM Conditions
Photon Rate per Second in 72 eV Band
1000
500
200
100
50
20
10
5.9
6.0
6.1
log(T) 5.8
Normal
Abundances
6.0
6.2
6.1
5.9
6.2
Depleted
Abundances
5.8
20
50
100
200
500
1000
Photon Rate per Second in 66 eV Band

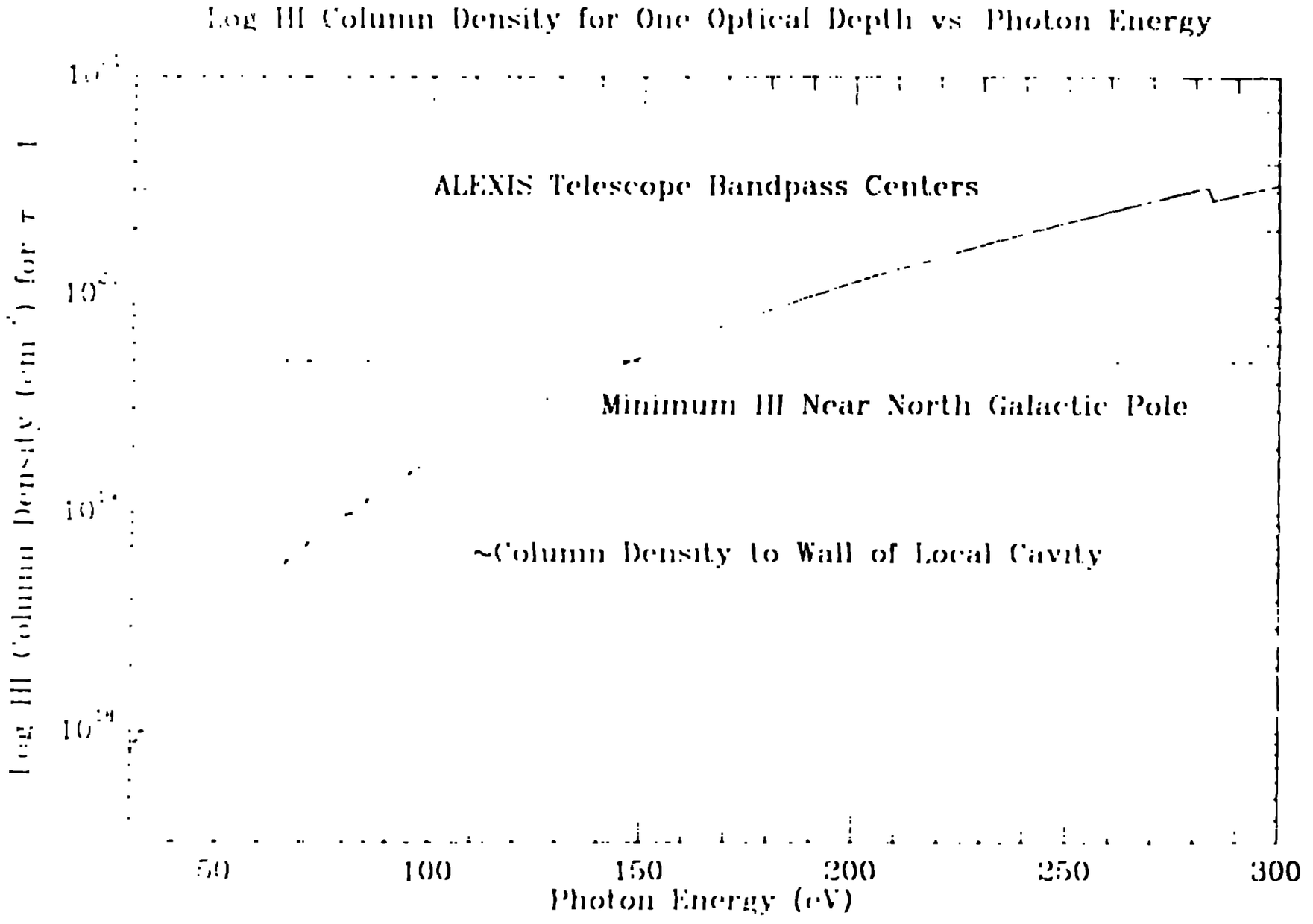
Log HI Column Density for One Optical Depth vs Photon Energy
ALEXIS Telescope Bandpass Centers
Minimum HI Near North Galactic Pole
~Column Density to Wall of Local Cavity
Log HI Column Density (cm⁻²) for τ = 1
Photon Energy (eV)
50
100
150
200
250
300

Figure 2

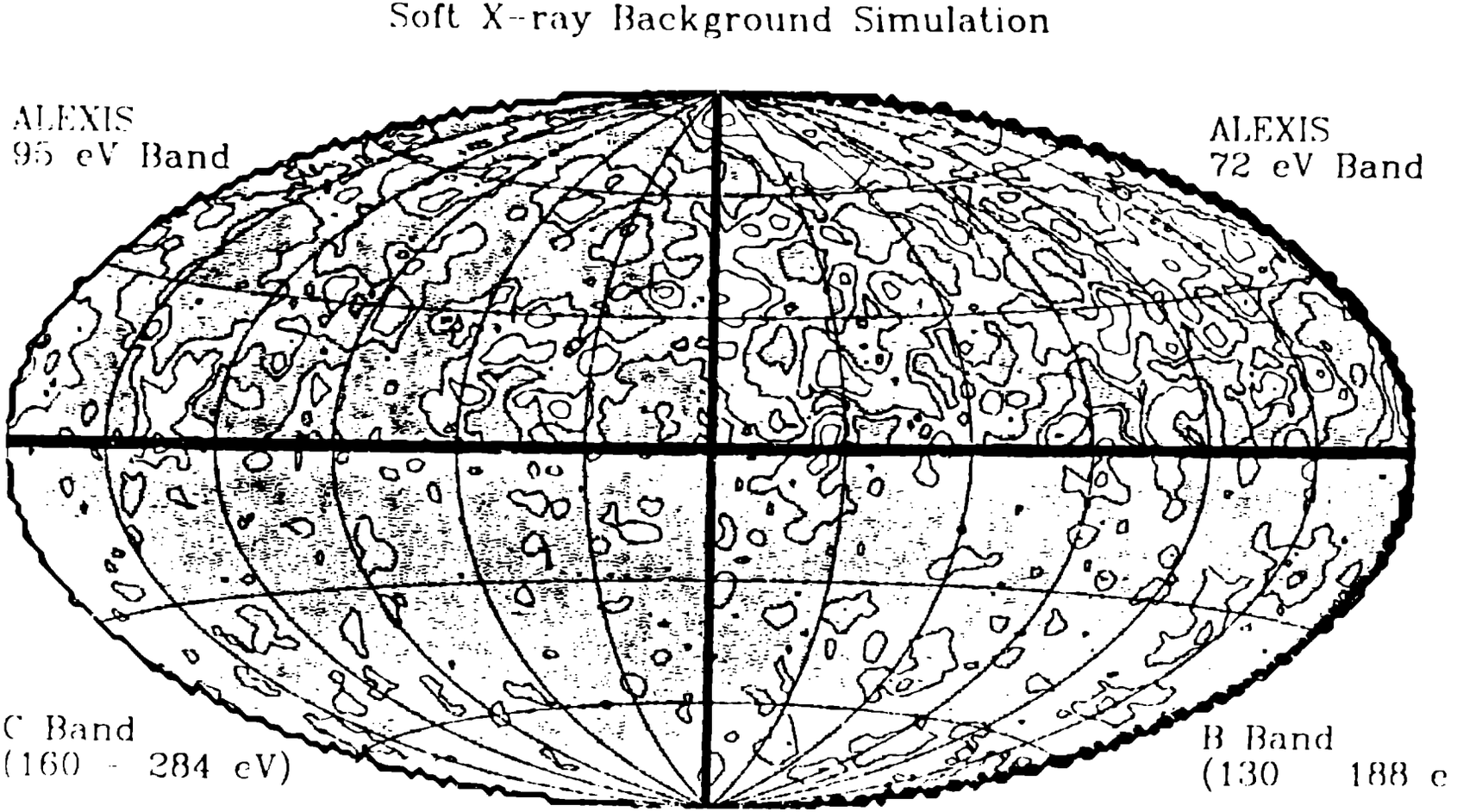
Soft X-ray Background Simulation
ALEXIS
95 eV Band
ALEXIS
72 eV Band
C Band
(160 - 284 eV)
B Band
(130 188 e

Figure 3